

LASER INTERFEROMETER GRAVITATIONAL WAVE OBSERVATORY
- LIGO -
CALIFORNIA INSTITUTE OF TECHNOLOGY
MASSACHUSETTS INSTITUTE OF TECHNOLOGY

Technical Note	LIGO-T1800224-v0	2018/07/09
Thermal State of LLO Test Masses: Mirror Degradation Monitor First Progress Report		
SURF Student: Guadalupe Quirarte, Harvey Mudd College Mentors: Carl Blair, Joseph Betzweizer		

California Institute of Technology
LIGO Project, MS 18-34
Pasadena, CA 91125
Phone (626) 395-2129
Fax (626) 304-9834
E-mail: info@ligo.caltech.edu

Massachusetts Institute of Technology
LIGO Project, Room NW22-295
Cambridge, MA 02139
Phone (617) 253-4824
Fax (617) 253-7014
E-mail: info@ligo.mit.edu

LIGO Hanford Observatory
Route 10, Mile Marker 2
Richland, WA 99352
Phone (509) 372-8106
Fax (509) 372-8137
E-mail: info@ligo.caltech.edu

LIGO Livingston Observatory
19100 LIGO Lane
Livingston, LA 70754
Phone (225) 686-3100
Fax (225) 686-7189
E-mail: info@ligo.caltech.edu

1 Introduction

The Advanced LIGO (aLIGO) detector is composed of a Michelson interferometer with 4 km Fabry-Perot optical cavities that function as the arms of the interferometer. These cavities utilize high-reflectivity fused silica mirrors that form an optical cavity and interact with high power laser beams. These mirrors are referred as the input test mass (ITM) and the end test mass (ETM) of each arm as shown below in Figure 1. Each cavity has an optical power that ultimately will reach 800 kW. A small portion of this power is absorbed by test masses and then converted into heat. A thermal transient is created in the mirrors when the arm cavities control systems are locked attaining optical resonance in the arm cavities.

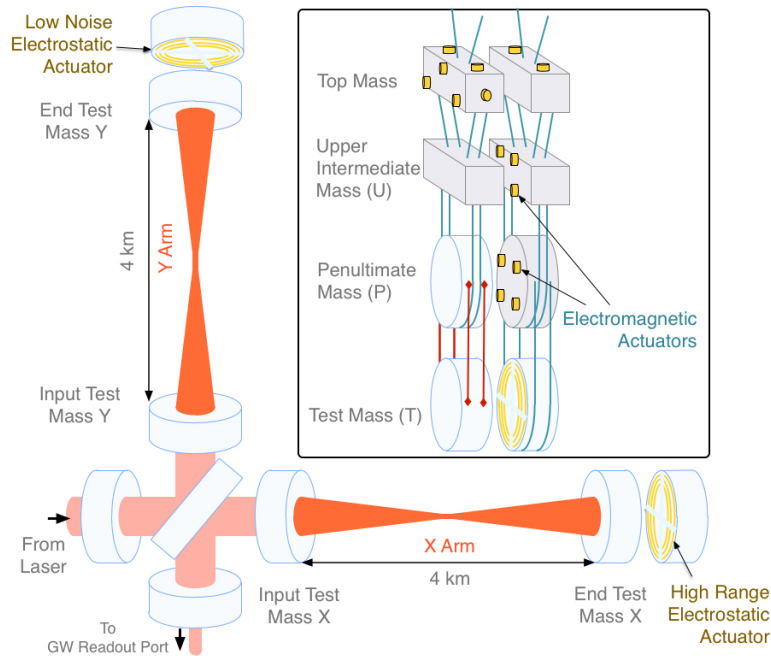


Figure 1: Diagram of an Advanced LIGO interferometer with Fabry-Perot cavities. [11].

This thermal transient's effect on the interferometer is dominated by two mechanisms. The first is known as thermal lensing which is caused by a change of refractive index through the thermo-optic effect. This thermal lensing can cause aberrations that contribute to a deterioration of the mode matching between the many optical cavities of the interferometer which in turn reduces the sensitivity of the interferometer.[2]

The second effect is the high-reflectivity coatings of the test masses being deformed from thermal expansion. A change of the radius of curvature (ROC) of the mirror is the first order deformation and this shifts the frequency of the transverse optical modes (TEM) resonant in the cavity. This changes the tuning conditions for parametric instabilities. As the mirror warms there is a relatively small increase in the mechanical mode frequencies due to the small positive thermal dependence of the Young's modulus of the mirror substrates. Parametric instabilities arise when the frequency spacing between the fundamental mode and a TEM mode equals the mechanical mode frequency. The interferometer can become inoperable and unstable if this condition is met.

These are problems that needs to be addressed and investigated. Work has been completed by LIGO researchers to design and develop strategies aimed to compensate these thermal effects such that they do not impact the detector sensitivity. The paper, Thermal modelling of Advanced LIGO test masses discusses how LIGO researchers have built a thermal model of the test masses that applies shifts in mechanical mode frequencies as a probe for the overall temperature of the mirror. This paper provides information on estimates of the coating absorption of the ETMY of the Livingston detector.[2]

LIGO researcher, Simon Tait, has worked with the thermal model outlined above in an effort to create an instantaneous absorption estimate of aLIGO test masses. He has modified the COMSOL thermal model and has written Matlab scripts that extract eigenfrequency and temperature data from the models. He has conducted parameterizations on the data to create an exponential model which he compared with experimental frequency tracking. The experimental frequency tracking integrates a transfer function and the extraction of the coating absorption. His final results focus on the month of July 2017 with a normalized change in frequency prediction. Covering both locked and unlocked states, his code calculates the coating absorption estimate by normalizing the gradient of the measured frequency shift data of each mechanical mode from the Optical Mode Cleaner (OMC) data. Shifts in the mechanical frequencies are tracked through this method during stable lock periods which must be more than 120 minutes.

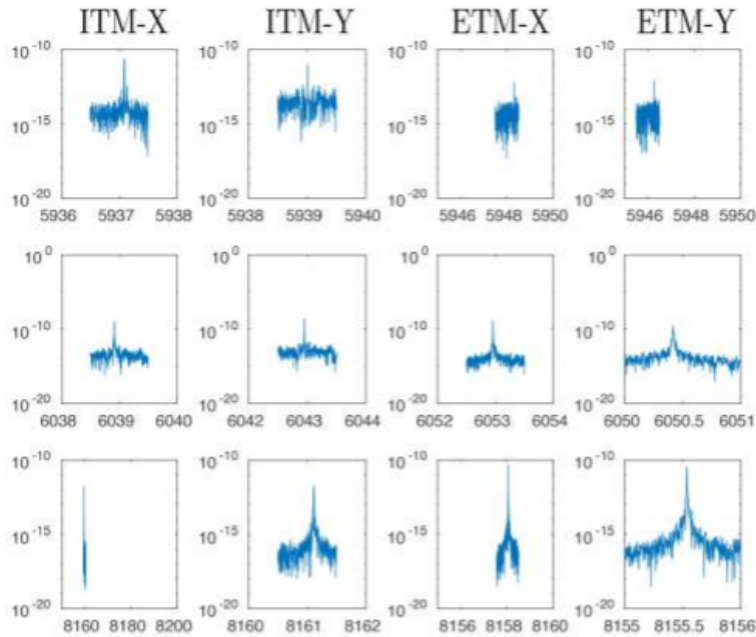


Figure 2: This is the windowed Power Spectral Density of the OMC output showing resonant frequencies of ITMs and ETMs in Hz. [1].

Due to time constraints involved with the amount of data needed to accurately track the shift of high-frequency signals, tests have only been conducted between January and September of 2017. [1] However, further work that can be integrated is implementing a Kalman Filter into the LLO Thermal Compensation System monitoring system to help

produce an instantaneous absorption estimate of the LLO test masses.[3]

1.1 Motivation

The purpose of this project is to use the eigenmodes of the test mass to measure its thermal state. I will build a Kalman filter to optimally estimate the eigenfrequencies of the test mass. I will be working with COMSOL models and learning how to analyze and extract useful information from them. I will also be using the LIGO CDS system that allows me to get data from the interferometer archives. Integrating the Kalman filter state space model parameters such as the test mass coating absorption can be inferred. This information will then be used to optimize the thermal compensation, to minimize detrimental thermal effects on the interferometer.

Currently, I have focused on analyzing COMSOL models and interferometer data so that I can design the state space model for the Kalman Filter. I have built on the existing COMSOL Multiphysics models from S.Tait [3] and H. Wang [2]. I have also parameterized the simulated eigenfrequency data in preparation for building a Kalman filter state space model.

In the following sections I describe the essential components of the thermal compensation system, introduce the finite element model and the parameterization that has been done.

2 Progress

2.1 Background

2.1.1 The Thermal Compensation System (TCS)

aLIGO's Thermal Compensation System (TCS) is supposed to help mitigate thermal lensing optical distortion effects.

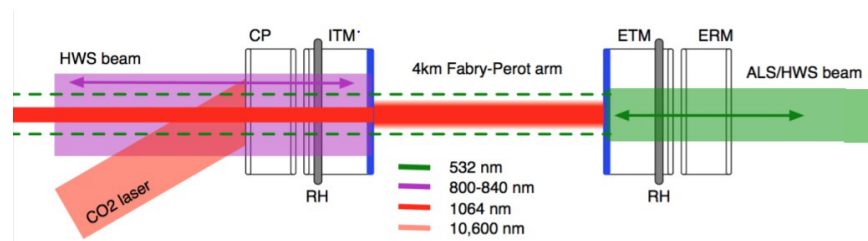


Figure 3: TCS system including ITM, ETM, circular ring heater (RH) to help heat the test masses on the outside, a CO_2 laser projects various annular shapes onto the compensation plates, and the Hartmann Wavefront Sensor (HWS) [3].

The RH heats the test masses on the outside near the rear surface. This produces a negative thermal lens in the optic and decreases the radius of curvature of the concave mirrored surface of the test mass. The CO_2 laser heats an area in the center of the compensation

plate, this produces a positive thermal lens. The HWS measures the wavefront distortion of the the HWS probe beam. This wavefront distortion is dominated by the thermal lens in the ITM and CP. The purpose of this system is to compensate for the laser power absorbed in the test mass mirror coatings. [1]

The power absorbed into the optic is proportional to the input laser power P_{power} and α_λ the absorption at one wavelength. The formation of a thermal lens and thermal expansion are the two effects created by the thermal transient that forms when the cavities control system is locked, this locking process will be described below. Figure 4 provides a visual of a the thermoelastic surface deformation and wavefront distortion due to the thermal lens. The thermally distorted mirror, illustrated as a dashed line, shows the change of radius of curvature of the mirrors. This shifts the frequency of the transverse optical modes (TEM) resonant on the cavity by the order of $10^3 Hz$. This can dramatically, change the tuning conditions for parametric instabilities, inducing many different instabilities. The change in temperature of the optic results in a small shift in the mechanical eigenmode frequency of the test masses of approximately 0.2 Hz. If the shifted frequency of the TEM modes and the spacing to the fundamental central mode of the cavity become equal to the frequency of the mechanical modes radiation pressure, then the radiation pressure of the optical modes can result in an exponentially increasing excitation of the mechanical modes known as parametric instability (PI) leading to the unlocking of the cavity. [1]

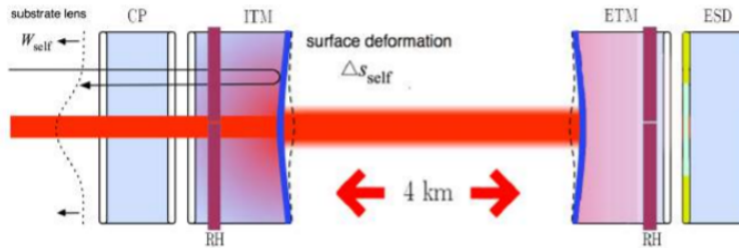


Figure 4: Thermoelastic surface deformation [3].

The cavities are locked through the Pound Drever Hall technique . A basic layout for locking a cavity to a laser is depicted below. This is the setup that permits to measure length noise in the cavity. The main mechanism behind the setup can be divided into three steps. A beam is sent into the cavity, a photodetector takes in the reflected beam, and then its output goes to a length controlling actuator. With a correct feedback setup, the system will hold at the length of the cavity where light is resonant. [10]

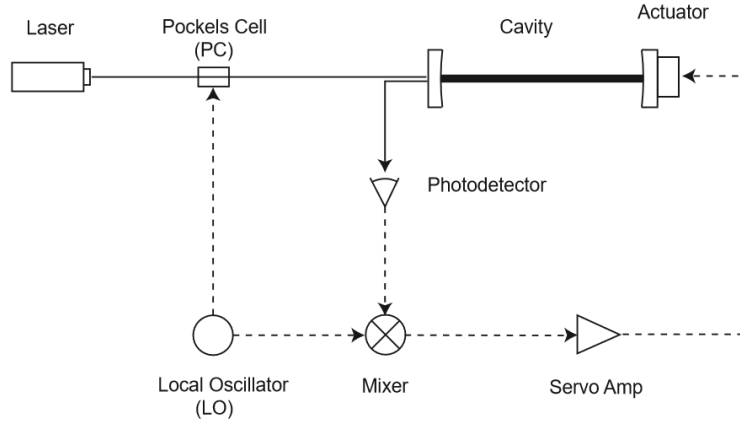


Figure 5: Locking a cavity to a laser. (Dashed lines are signal paths and solid lines are optical paths) [10].

When the cavity is resonant, it also experiences a large laser power build up. A portion of the light is absorbed in the high reflectivity optical coating. Currently, the detectors have design specifications for ETM coatings to have an optical absorption of 0.5 ppm and 99.999 reflectivity at 1064 nm. [1] The input mirror is more complicated as the reflectivity is formed by the ITM and another mirror PRM forming a coupled cavity. The resulting resonance results in 400x more light in the arm cavity compared to the input light. The small portion of this light that is absorbed in the coating dominates the thermal load on the test mass resulting in the deformation as pictured on Figure 4.

2.2 Final Element Model

2.2.1 Method

Mechanical mode frequencies can be described as test mass thermometers. They depend on the dimension of the test mass and on two material properties with a temperature dependence. These properties are the Young's modulus and the Poisson ratio. [2] An analytic way to express the eigenfrequencies of a cylinder is by following the equation below.

$$\omega_m = \beta_m \sqrt{\frac{Y(T)_{bulk}}{\rho(1+\nu)}}$$

Equation 1. The Mechanical Mode Frequency [3]

As shown above, the mechanical mode frequency ω_m is directly proportional to the square root of the Young's modulus $Y(T)_b$ and inversely proportional to the material density ρ and the Poisson ratio ν . The variable β_m is corresponding to a constant dependent on the geometry of the cylinder.

2.2.2 Thermal Model

A thermal model of the test mass allows the temperature distribution in the test mass to be estimated for a particular thermal load on the test mass. This thermal mode includes the

test mass and its surrounding bodies. The heat transfer model of aLIGO test masses can improve its accuracy by taking into account thermal coupling. This is done by including the radiative heat transfer between the test mass and the other bodies surrounding it, which are discussed in section 2.1.1 under TCS. [2]

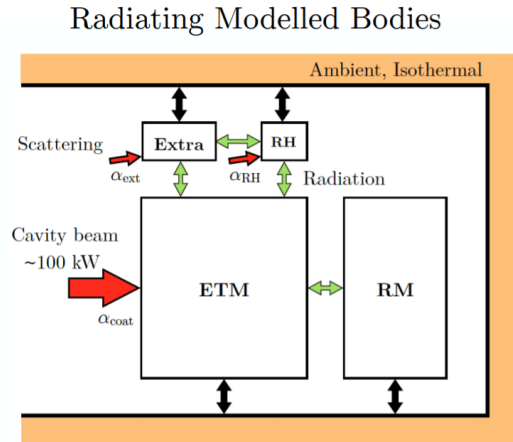


Figure 6: This is a heat transfer model between an end test mass and its surrounding elements, RH, RM, and the extra term represents other complex structures surrounding it. [3].

The model above illustrates the mechanisms involved during the transfer of heat when an arm cavity is locked. A portion of the light is converted into heat and scattered light from the beam covers bodies surrounding the test mass. Longer time constants are introduced to the test mass thermal transient because some of the heat from absorbed scattered light radiatively couples to other structures. This object's increased temperature then radiatively couples heat back to the test mass. [2]

2.2.3 COMSOL

To design a state space model of the test mass eigenfrequencies an accurate thermal model is required. I used COMSOL Multiphysics heat transfer toolbox to perform this thermal modelling. I modelled an end test mass, ETMY (test masses are nominally identical), and ran studies that pertained to its acoustic modes. An aLIGO test mass is a cylinder with a 170 mm radius and 200 mm thickness made of Heraeus Suprasil 3001 fused silica. [4] When a 100 kW laser beam is shot at the system, the model utilizes a heat source boundary condition with a Gaussian profile to simulate the area in which the beam hits the mirror surface as shown in figure 10. With a laser beam of this power, the coating absorption of 1 ppm would correspond to a total absorbed energy of 0.1 W. Figure 7 depicts the inputs and outputs of this thermal model and figure 8 provides a visual of the 2 dimensional thermal model of the whole system. [2]

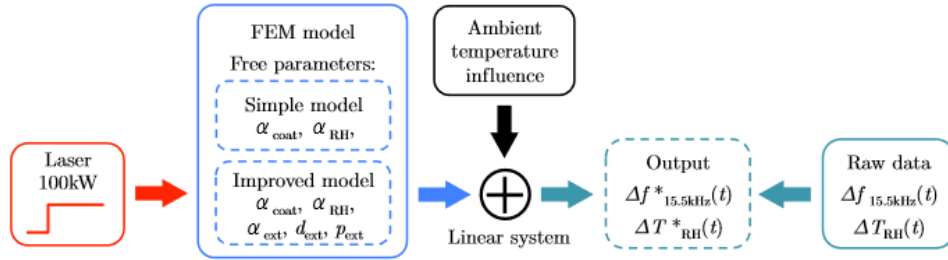


Figure 7: A finite-element model showing the inputs, outputs, and the free parameters to take into account when modelling a test mass. [2].

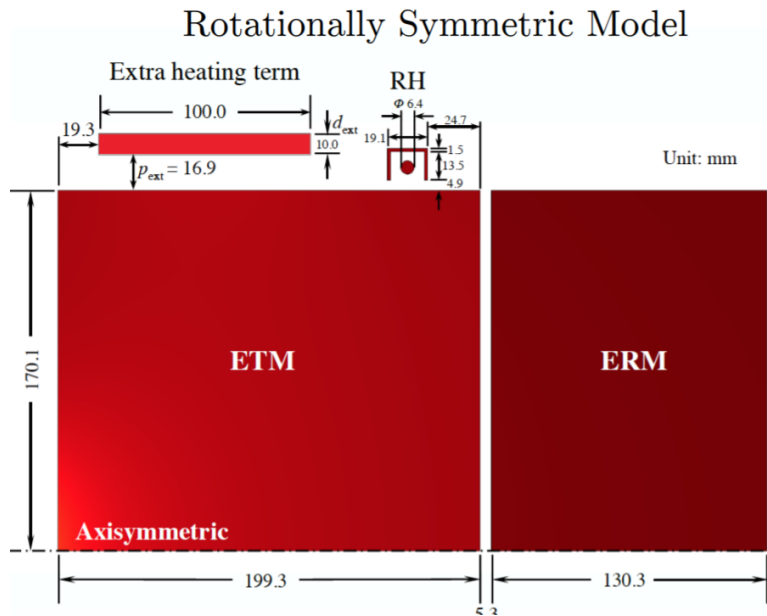


Figure 8: This shows the full dimensions of the 2DAS model, including scattering contribution (Extra Heating Term) Term [1].

By running the physics, setting the material properties, and running a time dependence and eigenfrequency study, H. Wangs [2] model was used as a guide to learn how to navigate through the program. I focused on testing the behavior of fused silica. It is a material with a unique behavior as its Youngs modulus has a temperature dependence. This causes the rise in frequency of the mechanical modes of the material. Below is a table of the material properties modelled for this material.

Material Property	Symbol	Fused Silica	Unit
Density	ρ	2203	$\frac{kg}{m^3}$
Poisson's Ratio	ν	0.17	1
Young's Modulus	E	$(7.3 \times 10^{10})(\Delta T)$	Pa
Thermal Conductivity	κ	1.38	$\frac{W}{mK}$
Thermal Expansion Coefficient	α	5.5×10^{-7}	$\frac{1}{K}$
Heat Capacity	C_p	740	$\frac{J}{kgK}$
Relative Permittivity	ϵ	3.8	1
Electrical Conductivity	σ	1×10^{-14}	$\frac{S}{m}$
Surface Emissivity	ϵ_e	0.93	1

I conducted a thermal modelling simulation by adding a theoretical heating load on one of the faces of the test mass. I then conducted a time dependent study to observe how the model heated up by the Boundary Heat Source. Afterwards, I directed a study on eigenfrequencies and found the eigenfrequency values that gave depictions of the mode shape of the model. When an object is vibrating with a certain eigenfrequency (natural frequency), the structure of the object deforms into a corresponding shape. The COMSOL three dimensional visual of the mode shape is an exaggeration of the deformation, but it provides us a geometrical understanding of the eigenmode. An eigenfrequency analysis provides the shape of the mode, but the actual size of the deformation can only be determined with the knowledge of an actual excitation with damping properties. With the implementation of heat transfer physics to understand the effect the shooting of the high-power laser beam had on the model, I was able to model the thermal transient formed. To extract the eigenfrequency information from the time depend dependant thermal analysis output the COMSOL MATLAB interface was required.

The thermal model includes the end test mass (ETM), reaction mass (ERM), and the ring heater (RH). Figure 2, illustrates these components which form part of the TCS. The geometry of the model is simplified to be a 2-dimensional Axis-symmetric representation of the system in order to avoid high computational demands that would be present while running a realistic geometry. This axis-symmetric model required heating loads including the main interferometer beam being axis-symmetric which is adequate for the current analysis. Moreover, optical absorption of the coating and scattering from the surrounding suspensions can also be implemented without the burden of having them exponentially increasing the solution time. However, this model is restricted to only monitor circularly symmetric mechanical eigenmodes. There is historic LIGO data containing the eigenfrequencies of 5.9, 6.0 and 8kHz modes. These modes have been analyzed with a 3D geometry model. The 5.9 and 6.0kHz modes are not axis-symmetric. The 8kHz mode is axis-symmetric, as a result the rest of this report will focus on the 8 kHz mode.

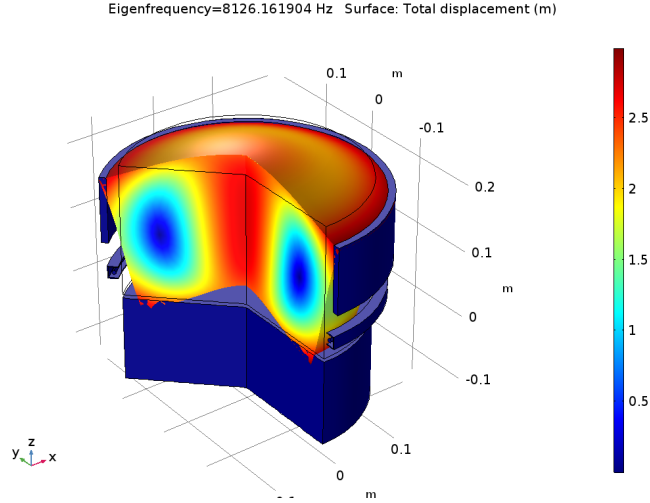


Figure 9: Mechanical mode shape of the 2DAS modelled ETM surrounded by the Ring Heater, ERM and an approximated suspension. [1].

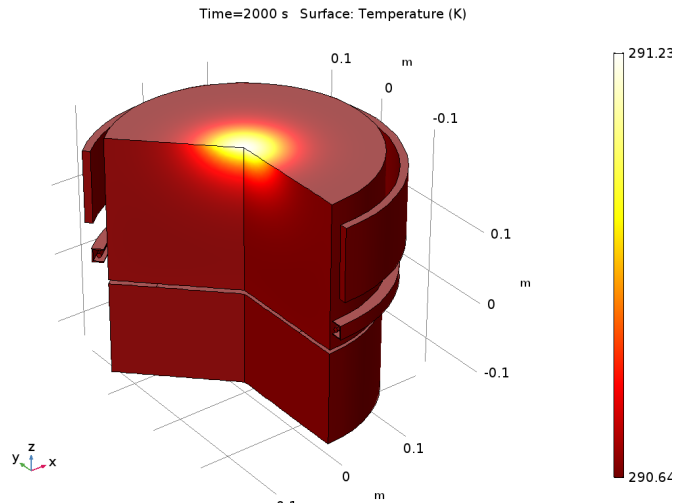


Figure 10: The change in the color has a radially outward changing direction which depicts the radial temperature gradient of the optic. [1].

An aLIGO interferometer's arm cavity contains a 750 kW Gaussian beam centered in the cavity. The equation below shows how the power absorbed by the optic, P_α , is calculated. The ω corresponds to the beam radius of the incident Gaussian light source and the value is 6.2 cm, the r refers to the distance from the center of the beam. P_{in} is the power input into the Fabry Perot cavity, k_{PRC} is the gain of the power recycling cavity, and k_{AC} is the gain from the arm cavity.[1]

$$P_\alpha = \frac{2(P_{in}k_{PRC}k_{AC})}{(\pi\omega^2)} \exp\left(\frac{-2r}{\omega^2}\right) \frac{1}{\alpha_c}$$

Equation 2. Power absorbed by the optic [1]

The α_c is the absorption of the coating on the test mass and it has been measured to be approximately 1.4 ppm at 1064 nm by using a Hartman Wavefront Sensor (HWS) for ETMY.[1] Furthermore, while analyzing the model, I noticed how the shift in ETM mechanical mode frequency was observed with relation to the surrounding optics in over 40 hours. By adding more components to the simulation this produces an elevation in re-radiation effects from the addition of these bodies. As a result, there is an increase in the calculated change in frequency over time [1].

3 Results

3.1 Model Parameterization

With a clear understanding and analysis of COMSOL, I rederived the curve fitting exponential model described in S. Tait [1]. By using MATLAB to obtain the COMSOL data of the eigenfrequency shift of the specific eigenmode 8.126 kHz, one can obtain the modelled shift of the frequency.

The equation below is the fit for frequency change in temperature calculated with COMSOL. This is a single term exponent with respect to time. The A corresponds to the total change in frequency, b is the model time constant, and c is the frequency at room temperature. This model can then be used to produce a simulated absorption estimate.

$$A(1 - e^{-bt}) + c \quad \text{Equation 3. Exponential Model [1]}$$

Before extracting the data through the MATLAB interface, I changed the COMSOL model by removing the frequency shift produced by heating and cooling and only kept the heating transient which would simulate a locked state. This was done by disabling the laser switch step function and an interpolation. The model was clarified by adding descriptions to the parameters and variables to understand how each one was derived. By removing the cooling transient, one could obtain a set of frequencies for a specific eigenmode. Simon's code produced an estimate for the change in temperature and frequency with self-heating from his pre-solved COMSOL model. Before extracting the eigenfrequencies, I extracted the temperature difference from the model for all the ETM points and plotted it to see if I observed a reasonable behavior representative of the heating. The graph below illustrates the heating transient formed for all four bodies modelled.

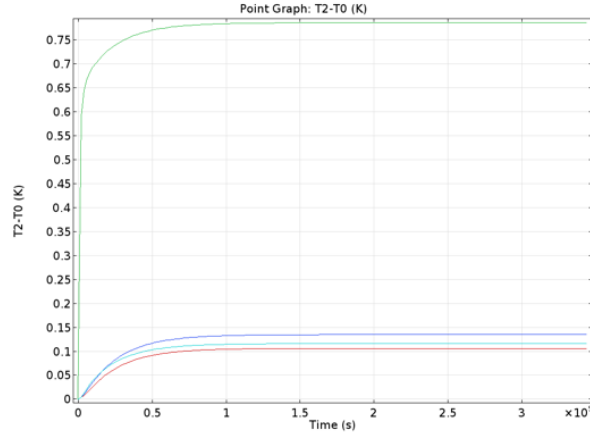


Figure 11: **Graph 1:** The graph above can be obtained by plotting on MATLAB the temperature over time of the end test mass and the other bodies to observe the behavior to model the heating of the masses. . [1].

Once I finished plotting Graph 1, I ran the loop through the data for the specific eigenmode. I then applied the curve fitting tool from MATLAB to work on fitting the analytical data to a second-degree exponential model to see if it provided a better fit to the data. As explained in section 2.2.2, thermal coupling must be taken into account when creating a thermal model. As a result, I decided to change the model to see if longer time constants are introduced. This could represent how some of the heat from scattered light radiatively couples to other elements.

$$A(1 - 2e^{-bt} + e^{-2ct}) + d \quad \text{Equation 4. A Test Exponential Model}$$

The gain A was approximately 0.09, the time constants b and c were 0.159 and 0.079, and d the eigenfrequency at room temperature was 8126. While fitting the model I made sure to keep the lower and upper limits large to ensure I was not forcing the data to fit a specific mold. Although the goodness-of-fit statistics obtained for both this model and the original model were very similar and the r squared was approximately 0.9936-0.9958, the first data point at time zero did not match the exponential model. By forcing d to be the y -intercept value of 8126.17, this would result in a less fit model of the function and would require a forcing of the variables b and c .

Below is a graph of the curve fitting model. With the value obtained for b and c , it is evident that c is very closely equal to half of the value of b . As a result, it can be simplified down to the previous exponential model while still maintaining closely similar values for the goodness-of-fit statistics.

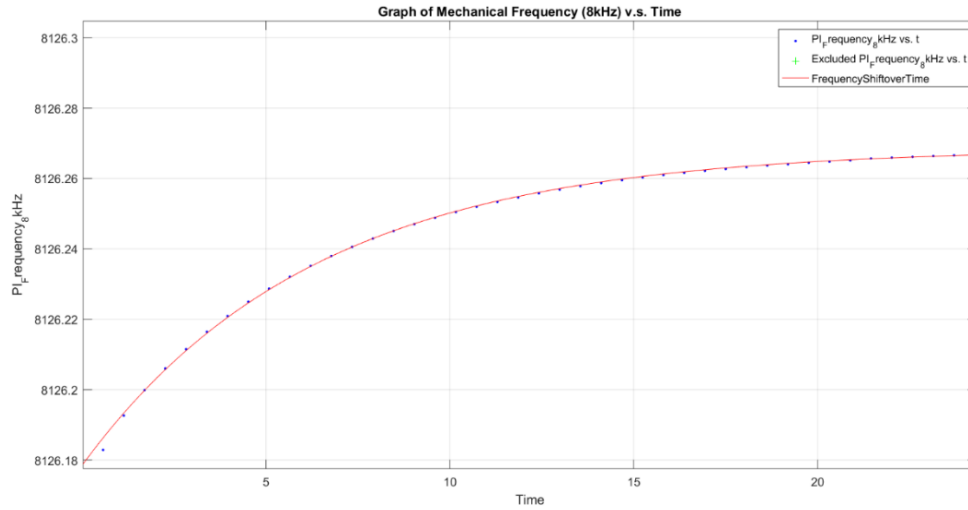


Figure 12: **Graph 2:** Exponential Model curve fitting of the analytical data from COMSOL. [1].

3.2 Calculated Coating Absorption

This section focuses on the results obtained for the period of January through September 2017 with estimates of the coating absorption. [1] The project does not focus on continuing the eigenfrequency tracking, but rather on understanding the technique used to extract the coating absorption as calculated in the graphs below.

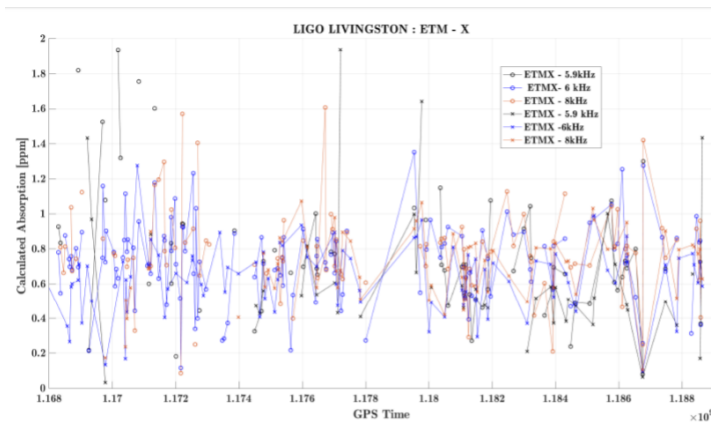


Figure 13: The calculated optical absorption during locked and unlocked states of ETMX between January and September of 2017. o refers to locked times and x is the interpolated estimate for the unlocked states. [1].

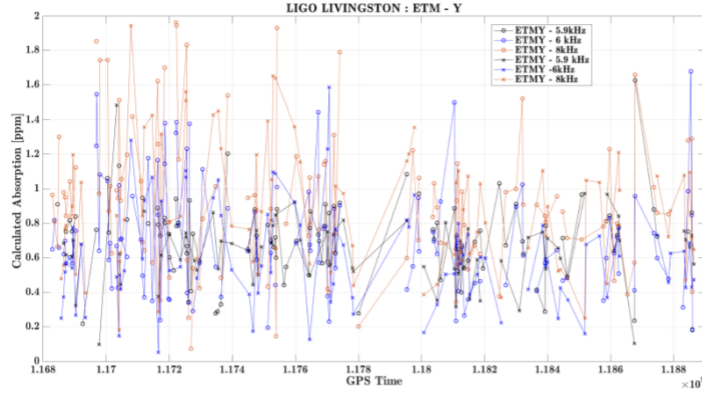


Figure 14: The calculated optical absorption during locked and unlocked states of ETMY between January and September of 2017. o refers to locked times and x is the interpolated estimate for the unlocked states. [1].

A prediction of the coating absorption was conducted, using the equation below,

$$\alpha_{coat} = \frac{\Delta f_{meas}}{\Delta f_{sim}} \alpha_{sim}$$

Equation 5. Coating Absorption [1]

where the numerator is the gradient of the measured frequency shift with time and it takes into account both locked and unlocked states. The denominator is the simulated change in frequency. This is multiplied by a scaling factor that takes in the HWS measured absorption of ETM and the power state of the interferometer. The code to complete this coating absorption estimate was run for the month of July and the approximation was accurate. It can then be used to model both the end and inner test masses, but as explained in the introduction due to time constraints the method was only implemented during the months of January and September 2017.[1] However, although the continuation of the project requires the understanding of the coating absorption extraction from the observable data, it will focus on the use of a different method to help monitor the system and extract coating absorption through a Kalman Filter.

4 Future Work

Moving forward, my project will begin to focus on transitioning into the theory and creation of a Kalman Filter for this system. The next weeks will be dedicated to creating state-space variables, a state-propagation matrix, a control-input model, and a final model and outputs.

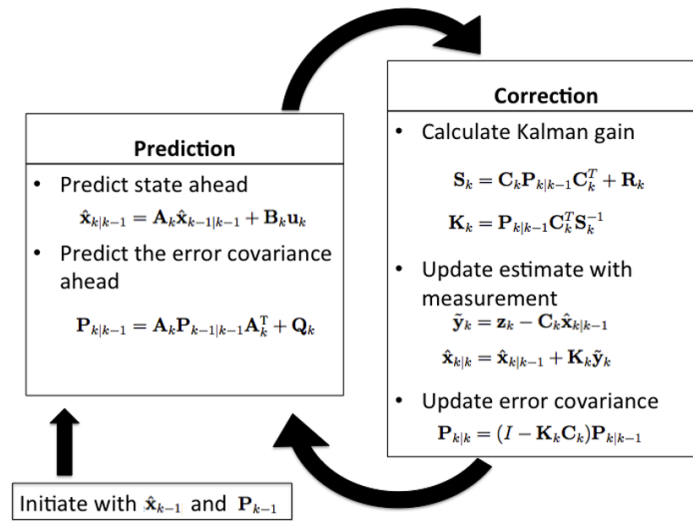


Figure 15: Kalman Filter thinking process. [5].

A Kalman Filter is a recursive algorithm that takes in as input a model and measurements to output less noisy and more accurate estimates. This filter is ideal for real time problems since it has the advantage of only taking in the previous state of the system and not requiring any other history. The figure above provides a clear overview of the mechanism behind the algorithm and its functionality. It is widely used in different areas such as navigational systems, guidance, and controlling vehicles. [5] The following steps outline an approach towards building a Kalman Filter. These are the steps I plan on conducting while moving forward in the project. [6]

- 1. Understand the situation:** Look at the problem and break it down to the mathematical basics.
- 2. Model the state process:** Starting with a basic model, it may not work effectively at first, but this can be refined later.
- 3. Model the measurement process:** Analyze how you are going to measure the process.
- 4. Model the noise:** This has to be completed for both the state and measurement process. The base Kalman filter assumes Gaussian (white) noise, so make the variance and covariance (error) meaningful (i.e., make sure that the error you model is suitable for the situation).
- 5. Test the Filter:** Observe the behavior of the filter.
- 6. Refine the Filter:** Try to change the noise parameters, if necessary go back and rethink the situation.

[6]

I have implemented a practice Kalman Filter tracking the position of an object using Matlab. I plan on extracting the velocity or acceleration from the system to simulate the extraction of coating absorption from the project Kalman Filter.

5 Conclusion

Overall, these past three weeks have been insightful and have given me a clearer understanding of the scope and the steps I should take to continue working on this project. I have met challenges while learning how to work with COMSOL and applying the Matlab interface to extract data. Most of my challenges have been technical while trying to navigate and read Matlab code. I have also met the problem that the current model may not be the best fit for the analytical data from the COMSOL models. Ideally, we would have liked the exponential model to have a better fit to the initial data points, but I will work with it and take this into account when transitioning into the next phase.

I anticipate to continue working on my analytical skills while also working on navigating, reading, and writing Matlab code in order to enhance my understanding of the control system theory behind the Kalman Filter. I expect to face technical challenges, but I will work on time management to mitigate the problems. I will construct weekly plans to help guide me towards initially completing a simple Kalman Filter and then slowly adding to it to make it more complex and applicable to the real scenario. It should take in the noisy eigenfrequency measurements and the exponential model and outputs a more accurate and precise estimates of the system. The model must take in the control variable of laser power and if this model functions properly, I will continue to expand on it and add other variables such as the ambient temperature's role in the shifts. Then I will have to generate a code that will help extract the coating absorption from the Kalman Filter by following the same technique previously followed. Challenges I may come across are having too noisy data that can be problematic to use for the Kalman Filter. Creating a filter that is either over or under fitted based on the way I decide to construct the state space model. These are the reasons why testing the model will be crucial to have an earlier sight of problems that can come across the project.

References

- [1] S. Tait, *An Instantaneous Absorption Estimate of aLIGO Test Masses*. pgs. 1-26 (2018).
- [2] H. Wang, C. Blair, M. Dovale Alvarez, A. Brooks, M. F. Kasprzack, J. Ramette, P. M. Meyers⁶, S. Kaufer, B. O'Reilly, C. M. Mow-Lowry, A. Freise. , *Thermal modelling of Advanced LIGO test masses..* Class. LIGO Document. 26 Apr (2017).
- [3] S.C. Tait, I.W. Martin, C. Blair, R. Jones Z. Tornasi, A. Bell, J. Steinlechner, J. Hough,S. Rowan. *Optical Absorption of Ion Plated Coatings and Instantaneous absorption at LLO.* [https : //dcc.ligo.org/DocDB/0150/G1800531/001/LVC2018.pdf](https://dcc.ligo.org/DocDB/0150/G1800531/001/LVC2018.pdf)(2018).
- [4] S. Tait, *Thermal Modelling*. LIGO COMSOL models.
- [5] G. Valdes, *Data Analysis Techniques for LIGO Detector Characterization*. University of Texas at San Antonio (2017).
- [6] Kalman Filter Tutorial, *Water Tank Sample Tutorial*. University of North Carolina (2018).
- [7] COMSOL, *The Heat Transfer Branch*. 709745 ISSN 02608774 (2012).
- [8] A. Brooks, *Pure state space model of thermal effects*. LIGO-T16xxxx-v1-D (2018).
- [9] Mathworks, *Kalman Filter Example*. (2018).
- [10] E. Black, *Notes on the Pound-Drever-Hall technique*. LIGO-T980045- 00- D (1998).
- [11] Abbot B.P., and LIGO Science Collaboration. "Calibration of the Advanced LIGO detectors for the discovery of the binary black-hole merger GW150914." Phys. Rev. D95, 062003 (2017). P1500248